TERM

REVIEW ARTICLE

Targeted Near-Infrared Fluorescence Imaging for Regenerative Medicine

Chengeng Yang[1] · G. Kate Park[1,2] · Eric J. McDonald[1] · Hak Soo Choi[1,2]

Abstract

BACKGROUND: Advances in tissue engineering and regenerative medicine over the last three decades have made great progress in the development of diagnostic and therapeutic methodologies for damaged tissues. However, regenerative medicine is still not the first line of treatment for patients due to limited understanding of the tissue regeneration process. Therefore, it is prerequisite to develop molecular imaging strategies combined with appropriate contrast agents to validate the therapeutic progress of damaged tissues.

METHODS: The goal of this review is to discuss the progress in the development of near-infrared (NIR) contrast agents and their biomedical applications for labeling cells and scaffolds, as well as monitoring the treatment progress of native tissue in living organisms. We also discuss the design consideration of NIR contrast agents for tissue engineering and regenerative medicine in terms of their physicochemical and optical properties.

RESULTS: The use of NIR imaging system and targeted contrast agents can provide high-resolution and high sensitivity imaging to track/monitor the *in vivo* fate of administered cells, the degradation rate of implanted scaffolds, and the tissue growth and integration of surrounding cells during the therapeutic period.

CONCLUSION: NIR fluorescence imaging techniques combined with targeted contrast agents can play a significant role in regenerative medicine by monitoring the therapeutic efficacy of implanted cells and scaffolds which would enhance the development of cell therapies and promote their successful clinical translations.

Keywords Regenerative medicine · Molecular imaging · Near-infrared imaging · Contrast agent

Chengeng Yang and G. Kate Park have contributed equally to this work.

✉ Hak Soo Choi
  hchoi12@mgh.harvard.edu

[1] Department of Radiology, Gordon Center for Medical Imaging, Massachusetts General Hospital and Harvard Medical School, 55 Fruit Street, Boston, MA 02114, USA

[2] Gimhae-Harvard Bioimaging Center, Gimhae Industry Promotion and Biomedical Foundation, 80-16 Golden root-ro, Juchon-myeon, Gimhae 50969, Republic of Korea

1 Introduction

The field of tissue engineering and regenerative medicine has made great progress over the last few decades along with the development of molecular imaging technology [1]. The goal of regenerative medicine is to develop an optimal treatment to restore tissues with limited regenerative capacities that have been damaged from trauma or disease, such as heart, bone, brain, muscle and nerve [2]. Different treatment approaches for regenerative medicine have been extensively studied and often involve the use of pluripotent stem cell administration, implantation of biomaterials, or gene stimulation for endogenous tissue growth [3, 4]. Although the efficacy of regenerative medicine is generally

accepted, monitoring of the treatment progression has been a major challenge. Consequently, regenerative medicine is still not commonly used in the clinic as the first line choice, and the mechanism of tissue healing and regeneration through these treatments is still not fully understood [5].

To overcome these challenges, many types of molecular imaging techniques have been utilized [6]. Figure 1 summarizes the progressive use of imaging modalities and contrast agents over the past 5 decades along with the growth of regenerative medicine in terms of monitoring and validation of tissue treatment. The traditional preclinical method for monitoring tissue growth is *ex vivo* histological analysis at various time points from different animals. This method requires a large number of animals and, thus, results in experimental errors from batch-to-batch variations. Noninvasive *in vivo* imaging techniques such as bioluminescence, positron emission tomography (PET), single photon emission computed tomography (SPECT), magnetic resonance imaging (MRI), and computed tomography (CT) have recently been used to monitor tissue growth noninvasively; however, their temporal and/ or spatial resolution are mostly limited [7]. Furthermore, most radiolabeled contrast agents used for functional molecular imaging to validate regenerated tissues have only been used to monitor the onset of vascularization [8]. Therefore, molecular imaging techniques that present fast-response but provide high resolution images are required to obtain longitudinal and quantitative tissue regeneration information in the same animal.

In this review, we discuss the use of near-infrared (NIR) fluorescent imaging technology along with targeted contrast agents to achieve real-time *in vivo* imaging of administered cells, scaffold degradation, and tissue growth. The NIR window (650–1700 nm) offers minimal background autofluorescence, reduced light scattering, and low tissue absorption, which together provide a high contrast ratio in the therapeutic area [9–12]. Thus, NIR fluorescence imaging can provide high resolution, high sensitivity, and a safe and cost-effective means of monitoring biological tissue to validate the efficacy of regenerative medicine [13–19].

2 Design of NIR fluorophores

Targeted contrast agents have recently been designed based on the novel concept of "Structure-Inherent Targeting" that combines imaging and tissue-specific targeting components into a single molecule [20]. The basic structure of a targeted contrast agent is composed of three domains: (1) imaging domain, (2) targeting domain, and (3) biodistribution domain. The imaging domain is used for tracking the fate of injected molecules and the targeting domain drives the agent to the target tissue. More importantly, the biodistribution domain contributes to reducing nonspecific background uptake and facilitate clearance from the body. This compact structural design enables the unbound contrast agent to be easily cleared from the body after tissue-specific targeting, thus reducing background signal and improving signal emitted from the targeted tissue. These exogenous contrast agents can be used to label cells,

Fig. 1 Summary of the imaging trends, modalities, and contrast agents in the field of tissue engineering and regenerative medicine
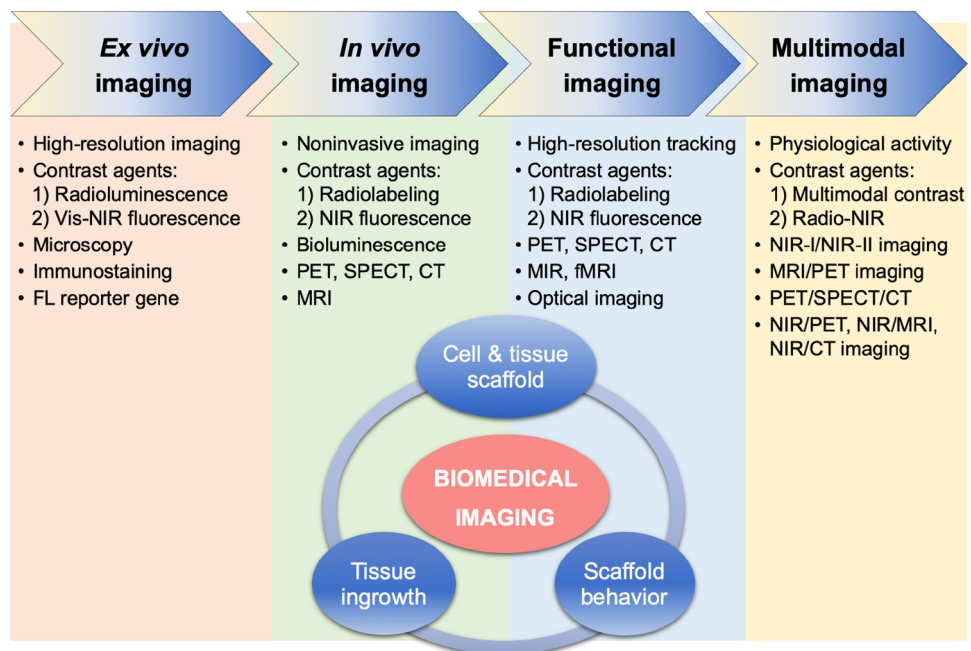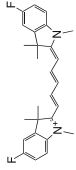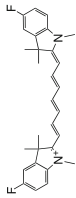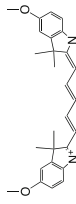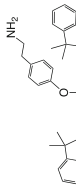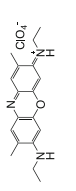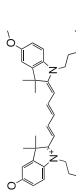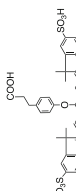
Table 1 Physicochemical and optical properties of targeted NIR fluorophores

NIR probe	T700-F	T800-F	ESNF13	CTNF126	Ox4	C700-OMe	P800SO3
Target tissue	Thyroid	Parathyroid	Mitochondria	Lysosome	Nerve	Cartilage	Bone
MW (Da)	419.53	445.57	443.60	612.87	395.84	615.91	988.23
LogD, pH 7.4	3.84	4.37	3.24	3.50	3.38	– 4.93	– 7.03
Abs max. (nm)	651	758	74	778	616	666	785
Em max. (nm)	665	771	700	790	635	692	802
ε (M^{-1} cm^{-1})	123,000	110,000	109,000	154,000	143,000	96,500	210,000
QY (%)	29.9	18.9	10.4	29.0	24.5	9.7	15.1
Chemical structure							
Refs.	[20]	[20]	[21]	[22]	[23]	[24]	[25]

Optical properties were measured in 100% serum, pH 7.4 at a concentration of 1–5 μM

In silico calculations of logD at pH 7.4 and total polar surface area were calculated using Marvin and JChem calculator plugins (ChemAxon, Budapest, Hungary)

MW molecular weight, ε extinction coefficient, *QY* quantum yield

scaffold, and target regenerated native tissues to gain detailed functional information.

Table 1 summarizes several representative NIR fluorescent contrast agents that have been used in tissue engineering and regenerative medicine. For instance, T700-F and T800-F are designed for targeting thyroid glands and parathyroid glands [20], ESNF13 is used for mitochondria targeting in living tissue [21], CTNF126 targets lysosomes in the subcellular region [22], Ox4 is specific to myelin membranes in nerves [23], C700-OMe is prone to stick to cartilage tissue [24], and P800SO3 shows high affinity to hydroxyapatite and calcium phosphate in bone [25]. In the following section, we discuss the relationship between the chemical structure of individual fluorophores and their physicochemical properties for specific tissue targeting and imaging in living organisms.

3 NIR fluorophores for live cell imaging

3.1 Longitudinal *in vitro* cell imaging

Cell-based regenerative medicine using different cell sources to promote tissue growth has been successful for the treatment of various diseases associated with heart, brain, and connective tissues [26]. In the case of damaged tissues, the therapeutic strategy involves administration of cells at the site of the injury to stimulate regeneration of damaged tissues and recovery of tissue function [12, 16]. Therefore, longitudinal tracking of administered cells is critical to monitor cell survival, integration, and proliferation in cell-based therapies. Many efforts have been made to develop molecular labeling agents to monitor cells and evaluate the progress of treatment [21]. However, current labeling techniques have many drawbacks. Direct cell labeling using magnetic nanoparticles often results in diluted signals with high cytotoxicity [21, 27, 28], and fluorescent protein transfection cannot provide sufficiently strong signals to detect the target tissue with high resolution [22, 29].

Therefore, molecular imaging contrast agents with high optical stability and low cytotoxicity are prerequisite for clinical use in the field of regenerative medicine. Kim et al. reported that lipophilic NIR fluorophores show efficient cellular uptake and can provide longitudinal cell tracking [21]. Figure 2 exhibits the 2D/3D chemical structure of ESNF13 and its optical properties with maximum absorbance and fluorescence emission around 700 nm in 100% FBS [21]. ESNF13 is composed of lipophilic cation polymethine backbone and exhibits high uptake in mitochondria with elevated intracellular stability (Fig. 2C). Since cells take up an excessive quantity of fluorophores at the initial phase, ESNF13 appears strongly in the cytosol
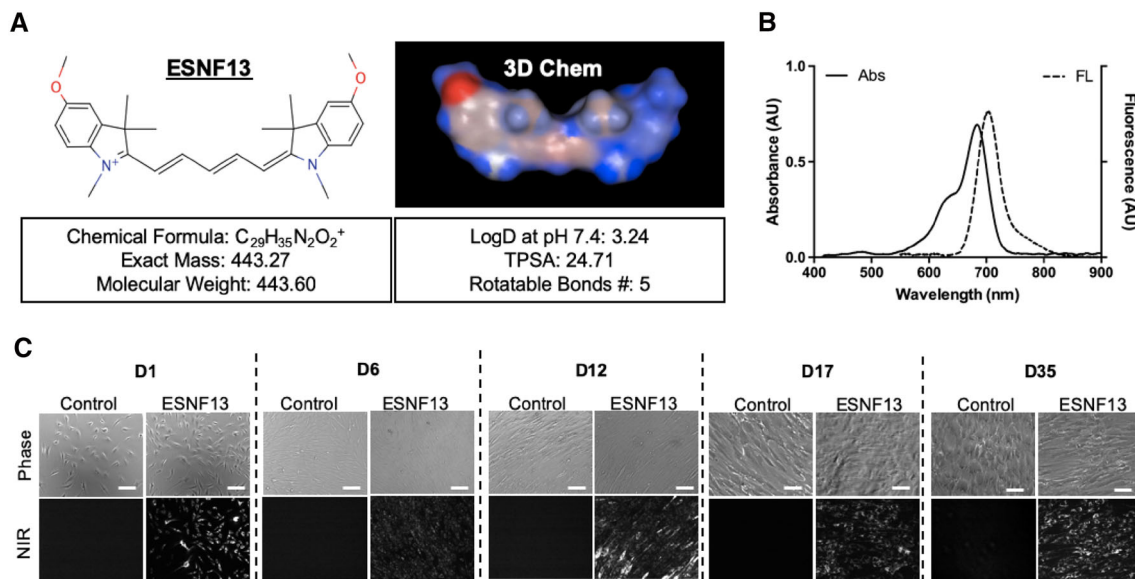
Fig. 2 Mitochondria targeting NIR fluorescent contrast agent. **A** Chemical structure and 3D structure of ESNF13. **B** Absorbance (solid line) and fluorescence emission (dotted line) spectra of ESNF13 in 100% FBS, pH 7.4. **C** Live cell imaging of ESNF13 (2 μM) in chondrocytes. Scale bars = 100 μm. All NIR fluorescence images have identical exposure and normalizations. Reproduced with permission from [21]

from Day 1 (D1) to Day 6 (D6) after cultivation. Cells then discontinue mitosis and start to differentiate, where ESNF13 is still maintained in the subcellular compartments up to Day 35 (D35), which allows longitudinal monitoring of cell proliferation and differentiation *in vitro* [21].

3.2 *In vivo* imaging of administered cells

Longitudinal tracking of administered cells followed by post-mortem *ex vivo* histological analysis is important to investigate the role of injected cells. However, it has been difficult to develop molecular contrast agents with high *in vivo* stability due to efflux and washout after cell staining. Recently, Park et al. reported lysosome-targeted fixable bioprobes and applied them in long-term tracking of transplanted lung tissue [22]. CTNF126 is an 800 nm emitting lipophilic cation possessing a primary amine, capable of labeling cells without interference of cellular activities. The lipophilic heptamethine core of CTNF126 allows passive diffusion across cell membranes and, at lower pH, the protonated primary amine holds CTNF126 inside the lysosome via ion trapping [30], enabling longitudinal monitoring of the implanted cells.

As shown in Fig. 3, cells labeled with both CTNF126 and IR786 (control NIR fluorophore) exhibited comparably high signals in the body for 5 min post-administration. However, the signal intensity of IR786 disappeared after 24 h, while CTNF126-labeled cells remained in high fluorescence, followed by signal migration from the lungs to liver. In addition, CTNF126 outperforms IR786 in terms of

chemical stability during harsh chemical processing of histological analysis, where hematoxylin and eosin (H&E) staining requires heating of specimens to at least 58 °C for over 1 h, then dipping them into strong organic solvents. Figure 3C represents that the signal intensity of CTNF126-labeled cells remained strong even after the harsh fixing process of formalin as well as H&E tissue staining. In conclusion, CTNF126 may be useful to label various type of cells to gain a better understanding of their *in vivo* and *ex vivo* behaviors after implantation [22].

4 NIR fluorophores for scaffold labeling

Biodegradable natural and synthetic polymer scaffolds are considered highly effective approaches applied in the field of regenerative medicine and tissue engineering [31–33]. To design optimal scaffolds, however, it is essential to make sure that the rates of scaffold disintegration and tissue ingrowth are congruent [34]. Therefore, various imaging techniques have been developed to track scaffold degradation longitudinally [35, 36]. As shown in Fig. 4, scaffolds with different polymeric backbones such as PLGA, PLLA, and collagen can be conjugated with zwitterionic NIR fluorophores to achieve noninvasive imaging after transplantation into the body [37–43]. The enzymatic degradation of scaffolds was able to be monitored at each time point without sacrificing animals or time-point sampling. The signal intensity at both implant sites of axilla and thigh significantly decreased over a period of time
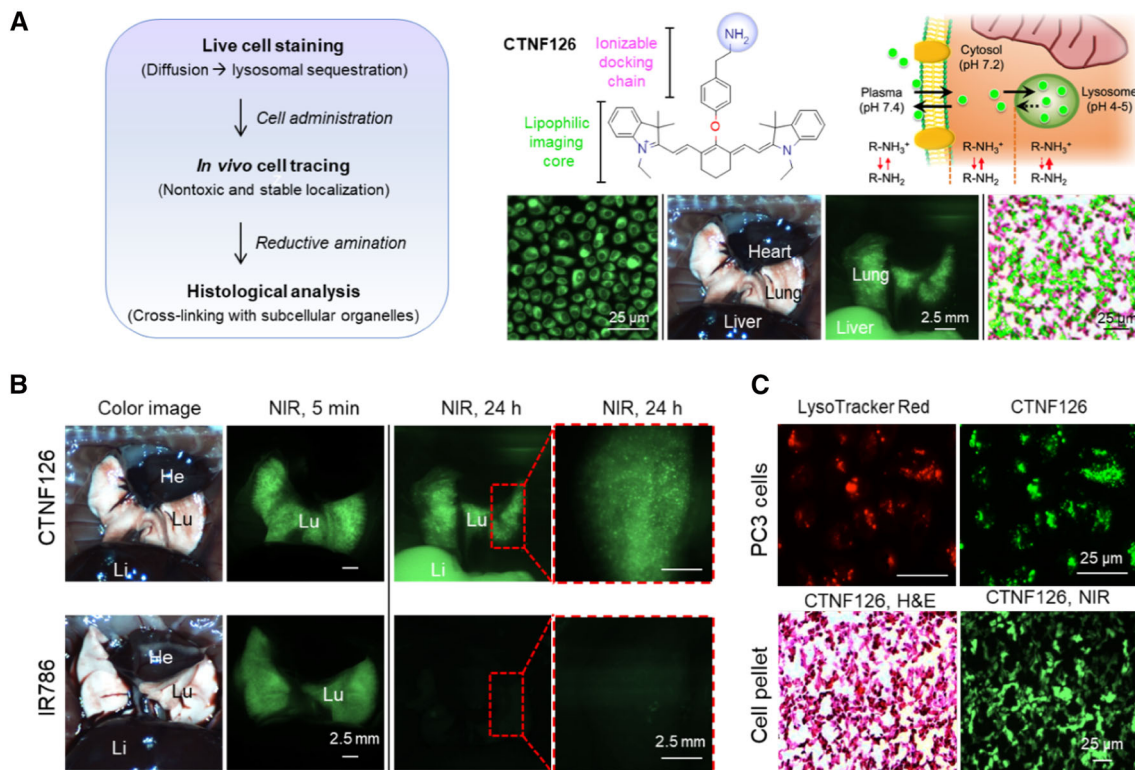
Fig. 3 Lysosome-targeted NIR fluorescent contrast agent. **A** Cell labeling and longitudinal tracking strategy of CTNF126 via lysosomal sequestration (ion trapping). The thickness of red arrow represents ionization tendency. **B** *In vivo* tracking of lysosomal fluorophore-labeled cells under the intraoperative NIR fluorescence imaging system. CTNF126 and IR786-stained cells were trapped in the lungs with strong fluorescent signals at 5 min post-intravenous injection. The cells labeled with CTNF126 were found in the liver as an evidence of cell migration from the lung capillaries at 24 h post-injection. **C** Lysosomal sequestration of LysoTracker imaged at 600 nm (top, left) and CTNF126 imaged at 800 nm (top, right). H&E and NIR imaging of cell pellets mimicking tissue structure labeled by CTNF126 (bottom). Reproduced with permission from [22]

from Day 3 (D3) to Day 28 (D28). These scaffolds were then removed from the animals, and H&E and NIR fluorescence images revealed both tissue ingrowth and scaffold degradation [44]. In conclusion, NIR fluorescence imaging can provide degradation profiles of scaffolds and tissue infiltration in real time without having to sacrifice animals.

5 NIR fluorophores for native tissue imaging

The human body is composed of muscular, nervous, epithelial, and connective tissues. Especially, connective tissue such as cartilage and bone is the most abundant in the body, and have limited regeneration capacities when damaged [45]. Nerve tissue injury is also one of the leading complications from surgery, often resulting in chronic pain and sensory loss. Regenerative medicine is used to promote the growth of damaged tissues and restore tissue function eventually. However, the mechanism behind the tissue regeneration is poorly understood because native tissue growth cannot be monitored without specific contrast agents to highlight the target tissue. Therefore, targeted contrast agents for real-time monitoring of the tissue growth process are prerequisite to evaluate the efficacy of treatment [46]. Generally, targeted contrast agents are designed via bioconjugation of a specific ligand on an imaging domain or vice versa [9, 10]. By incorporating one or multiple targeting moieties into the backbone of imaging domain, however, we can create new types of targeted contrast agents. Some examples of targeted contrast agents are reviewed in the following sections.

5.1 Cartilage-specific contrast agents

Cartilage is a connective tissue produced by chondrocytes and composed of 3 different structures including hyaline cartilage, fibrocartilage, and elastic cartilage [24]. Imaging of cartilage dysfunction using conventional imaging modalities such as MRI and CT are currently limited by their low resolution [24, 47, 48]. C700-OMe is a cartilage-specific NIR fluorophore displaying a superior signal-to-background ratio (SBR) value in real time from the nearby
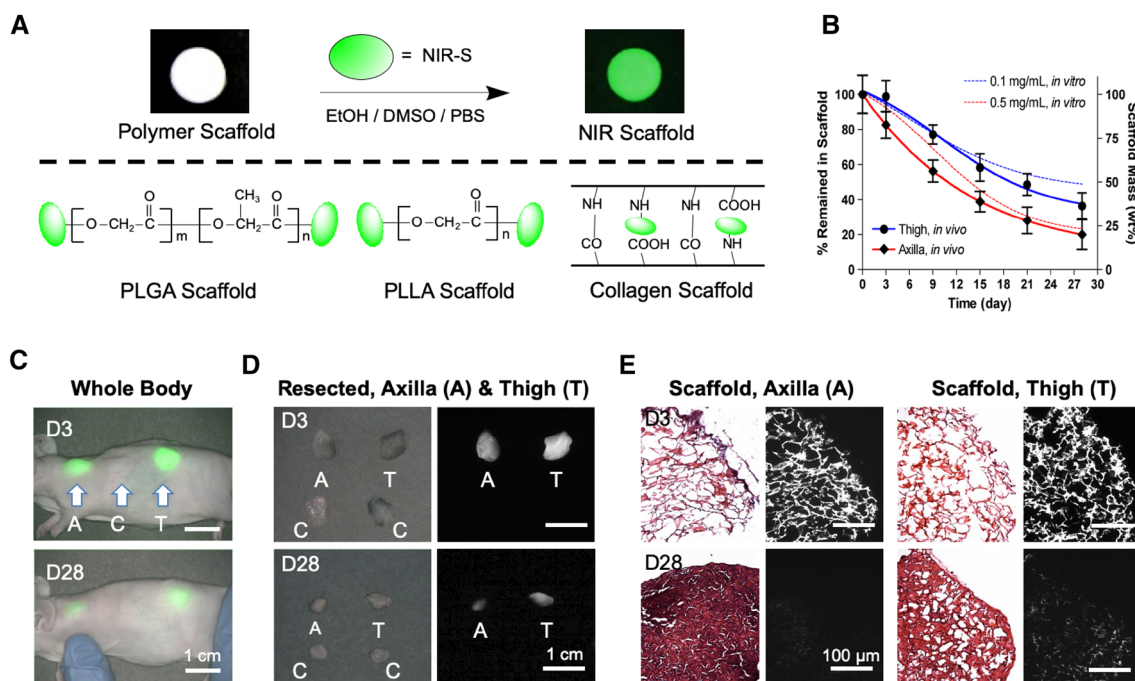
Fig. 4 Labeling strategy for biodegradable scaffolds with NIR fluorophores. **A** Schematic drawing of NIR scaffold preparation using NIR-S on the backbone of PLGA, PLLA, and collagen scaffolds. **B** Quantification of *in vivo* scaffold degradation in nude mice. Time course of signal changes in NIR scaffolds in animals (solid lines). *In vitro* test results were added as dotted lines for comparison. **C** Optical measurements of scaffold degradation by imaging NIR signals over the skin. *A* axilla, *C* control, *T* thigh. **D** Quantification of tissue ingrowth and scaffold degradation: NIR fluorescence imaging of resected scaffolds at each time point. **E** H&E and NIR imaging of resected scaffolds from (**D**). Scaffold degradation accompanying tissue ingrowth was compared. Reproduced with permission from [44]
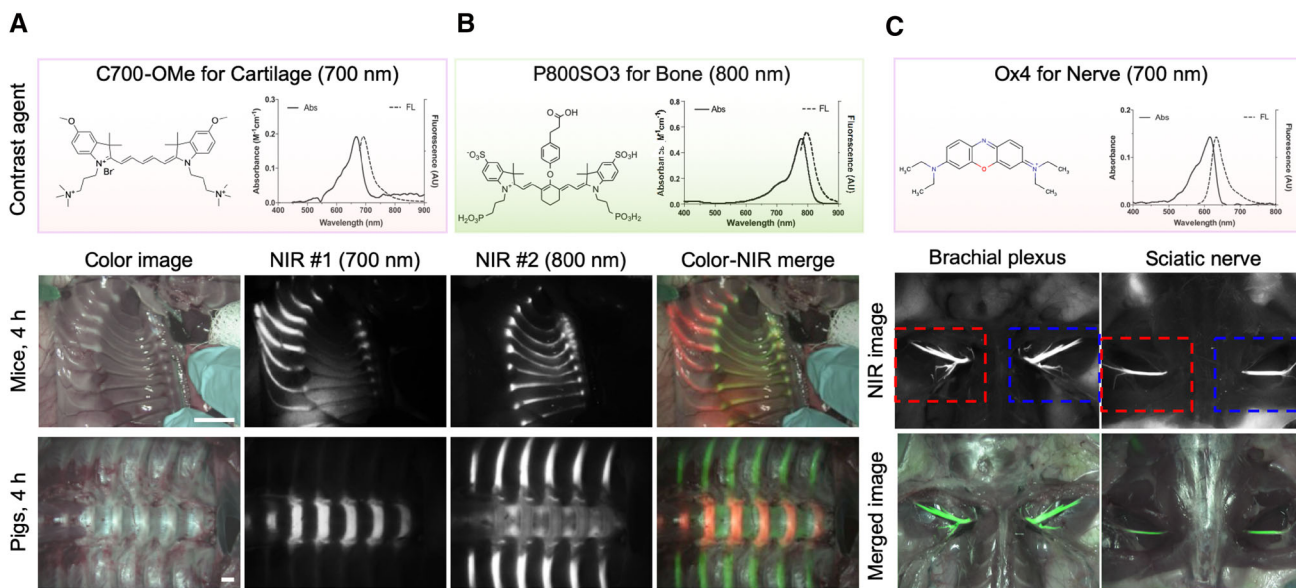

Fig. 5 A, **B** Tissue-specific targeting and imaging using NIR fluorescent small molecules. Chemical structure and optical properties of cartilage-specific C700-OMe and bone-targeted P800SO3, and their dual channel cartilage- and bone-specific imaging in mice (middle) and pigs (bottom). 0.4 mg/kg of each targeted fluorophore was injected intravenously into 25 g CD-1 mice and 35 kg Yorkshire pigs 4 h prior to imaging. Reproduced with permission from [24, 25]. **C** Chemical structure and optical properties of Ox4 (top) and its nerve-specific imaging in rats (bottom). 1 µmol of Ox4 was injected intravenously into SD rats 4 h prior to imaging. Reproduced with permission from [23]

bone [24]. The chemical structure of C700-OMe includes quaternary ammonium cations on a polymethine backbone (Fig. 5A). These permanent positive charges lead contrast agents to bind to cartilage tissues, mostly chondrocytes and acidic glycosaminoglycans, which was elucidated by injecting 20–400 μg/kg of C700-OMe intravenously into mice and pigs 4 h prior to imaging [24].

5.2 Bone-specific contrast agents

Although bone scans provide accurate diagnoses and tracking of bone diseases, the clinical outcomes of bone defects are challenging due to high complication and reoperation rates, in addition to poor functional outcomes [34]. There remains a lack of bone targeted contrast agents for better diagnosis and monitoring of the treatment efficacy of bone defects. P800SO3 is composed of bisphosphonates on a polymethine backbone, which makes it highly specific to minerals including hydroxyapatite and calcium phosphate [25]. P800SO3 exhibits a maximum emission wavelength around 800 nm, while P700SO3 shows a fluorescence emission at 700 nm (Fig. 5B). After a single intravenous injection at a dose of 0.4 mg/kg, P800SO3 showed highly specific affinity towards bones throughout the body including jaw, knee, and backbone in mice, rats, and pigs [24, 25]. P800SO3 also shows long-term stability in the target tissue, which could be ideal for

tissue regeneration because neoossification needs to be followed for several months [49].

5.3 Nerve-specific contrast agents

Although peripheral nerve axons readily regenerate to allow recovery of function after damage, myelinated nerves are particularly problematic as damage may lead to motor and sensory loss as well as chronic pain [23]. Nerves are often injured during surgery due to their small size and relatively unnoticeable appearance, and damage can be irreversible [23]. For imaging peripheral nerves, three types of nerve-binding agents have been reported: stilbene derivatives, distyrylbenzene (DSB) fluorophores, and styryl pyridinium (FM) fluorophores [50, 51]. Although these agents provide some degree of binding in the nervous tissue, impaired signal production is a paramount challenge due to relatively high tissue adsorption and scattering, as well as autofluorescence in the visible wavelength. Therefore, NIR fluorophores may serve as an optimal approach towards nerve imaging. Park et al. discovered nerve-specific NIR fluorophores that show instantaneous internalization to the multilayered myelin sheath and interaction with lipids in the myelin membrane. Figure 5C illustrates the chemical structure and optical properties of Ox4, of which absorbance and fluorescence emission wavelengths belong to 700 nm. A single intravenous
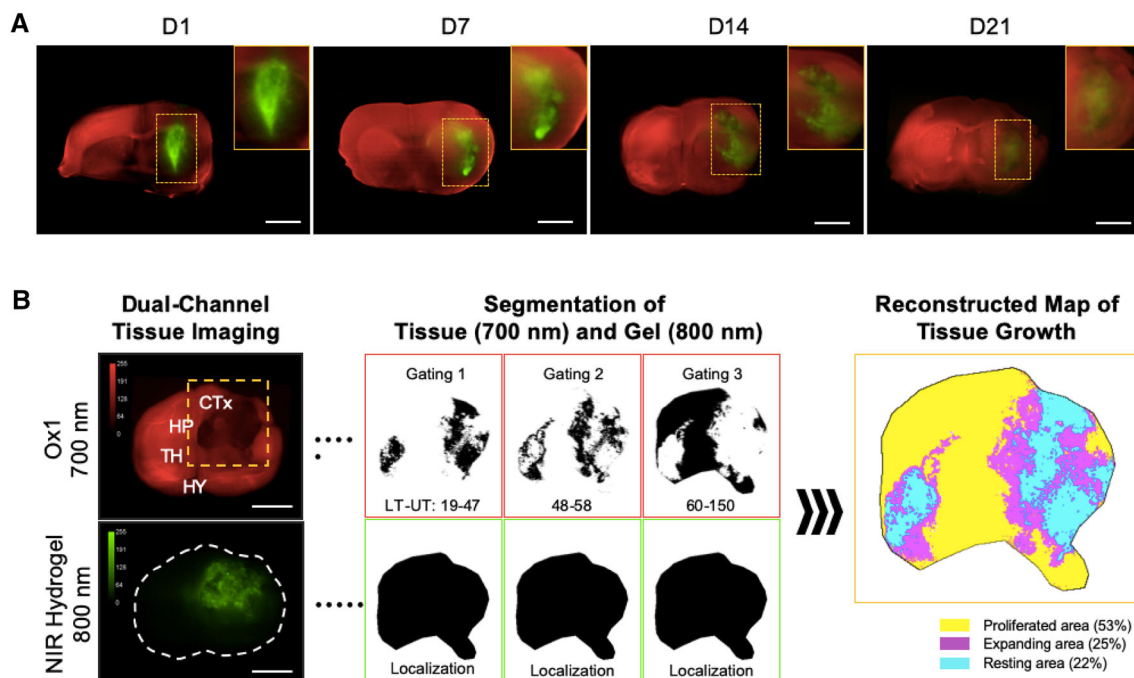

Fig. 6 Dual-channel imaging of brain tissue growth and NIR hydrogel degradation. **A** NIR hydrogel (20 μL) was injected orthotopically in the forebrain of CD-1 mice and Ox1 (100 nmol) was administered to the same animal an hour prior to imaging. Brain tissue ingrowth (red) and NIR hydrogel (green) degradation observed in the merged image. Sample thickness = 2 mm. **B** Spatial segmentation analysis of the NIR image for the quantification and visualized dynamic color mapping of the tissue ingrowth. Scale bars = 2.5 mm. Reproduced with permission from [46]

injection of Ox4 resulted in high uptake in the tiny branches of main nerves including brachial plexus and sciatic nerves [23].

6 Multispectral Imaging for tissue regeneration

Multichannel and multispectral imaging modalities are required in tissue regeneration to monitor both scaffold degradation and tissue growth simultaneously to make treatment plans more effectively. Very recently, dual-channel NIR fluorescent imaging of brain regeneration was achieved by using a 700 nm emitting blood–brain barrier (BBB)-permeable NIR fluorophore along with labeling the scaffold with an 800 nm emitting ZW800-3a [46]. As shown in Fig. 6, first, an injectable NIR hydrogel was synthesized by conjugating ZW800-3a on the backbone of gelatin scaffold, followed by crosslinking with hyaluronic acid (HA)–tyramine using recombinant tyrosinase. Then, BBB-permeable Ox1 was injected intravenously, enabling the monitoring of tissue ingrowth in the damaged brain. Figure 6A illustrates dual-channel monitoring of NIR hydrogel degradation and tissue regeneration up to 21 days. Images obtained from the two NIR channels (700 and 800 nm) were pseudocolored and merged to localize the tissue regenerated and scaffold degradation in the therapeutic area. The advantage of using high resolution NIR fluorescence imaging is that the regenerated area can be quantified based on the signal intensity. Figure 6B shows a reconstructed map of tissue growth providing a better understanding of the hydrogel treatment and the spatial segmentation analysis of the NIR image used for quantification of the tissue ingrowth [46].

7 Conclusions and perspectives

Regenerative medicine can provide therapeutic solutions for many unsolved problems in the clinic, and its potential has been growing along with the development of molecular imaging technology. Utilization of NIR fluorescence imaging and associated targeted contrast agents in tissue engineering and regenerative medicine can provide great insight in monitoring and quantifying the theranostic process of damaged tissue due to the high temporal and spatial resolution. However, current NIR fluorescence imaging in the NIR-I window (650–900 nm) is limited by the penetration depth in human tissue. To overcome this fundamental limitation, imaging in the NIR-II window (1000–1700 nm) has been actively investigated for noninvasive imaging of deep tissue due to the lower tissue scattering [52], which will enable monitoring of regenerative process more efficiently. Future researches should

focus on the development of multichannel and multispectral imaging, where three or more channels can be employed at the same time to elucidate the details in cell therapy, not only monitoring the treatment efficacy of cell-seeded scaffolds but also providing information on tissue growth, cell migration, and scaffold degradation simultaneously for better quantification. Overall, targeted NIR imaging approaches for tissue engineering discussed in this review have the potential to bring regenerative medicine a step closer to clinical translations.

Compliance with ethical standards

Conflict of interest All authors declare that they have no conflict of interest.

Ethical statement There are no animal experiments carried out for this article.

References

1. Santiesteban DY, Kubelick K, Dhada KS, Dumani D, Suggs L, Emelianov S. Monitoring/imaging and regenerative agents for enhancing tissue engineering characterization and therapies. Ann Biomed Eng. 2016;44:750–72.
2. Lin X, Huang J, Shi Y, Liu W. Tissue engineering and regenerative medicine in applied research: a year in review of 2014. Tissue Eng Part B Rev. 2015;21:177–86.
3. Zakrzewski W, Dobrzyński M, Szymonowicz M, Rybak Z. Stem cells: past, present, and future. Stem Cell Res Ther. 2019;10:68.
4. Zhang K, Wang S, Zhou C, Cheng L, Gao X, Xie X, et al. Advanced smart biomaterials and constructs for hard tissue engineering and regeneration. Bone Res. 2018;6:31.
5. Bt Hj Idrus R, Abas A, Ab Rahim F, Saim AB. Clinical translation of cell therapy, tissue engineering, and regenerative medicine product in Malaysia and its regulatory policy. Tissue Eng Part A. 2015;21:2812–6.
6. Kupfer ME, Ogle BM. Advanced imaging approaches for regenerative medicine: emerging technologies for monitoring stem cell fate in vitro and in vivo. Biotechnol J. 2015;10:1515–28.
7. Choi HS, Frangioni JV. Nanoparticles for biomedical imaging: fundamentals of clinical translation. Mol Imaging. 2010;9:291–310.
8. Nam SY, Ricles LM, Suggs LJ, Emelianov SY. Imaging strategies for tissue engineering applications. Tissue Eng Part B Rev. 2015;21:88–102.
9. Owens EA, Henary M, El Fakhri G, Choi HS. Tissue-specific near-infrared fluorescence imaging. Acc Chem Res. 2016;49:1731–40.

10. Owens EA, Lee S, Choi J, Henary M, Choi HS. NIR fluorescent small molecules for intraoperative imaging. Wiley Interdiscip Rev Nanomed Nanobiotechnol. 2015;7:828–38.

11. Gioux S, Choi HS, Frangioni JV. Image-guided surgery using invisible near-infrared light: fundamentals of clinical translation. Mol Imaging. 2010;9:237–55.

12. Lee JH, Park G, Hong GH, Choi J, Choi HS. Design considerations for targeted optical contrast agents. Quant Imaging Med Surg. 2012;2:266–73.

13. Hu S, Kang H, Baek Y, El Fakhri G, Kuang A, Choi HS. Real-time imaging of brain tumor for image-guided surgery. Adv Healthc Mater. 2018;7:e1800066.

14. Kang H, Hu S, Cho MH, Hong SH, Choi Y, Choi HS. Theranostic nanosystems for targeted cancer therapy. Nano Today. 2018;23:59–72.

15. Kang H, Mintri S, Menon AV, Lee HY, Choi HS, Kim J. Pharmacokinetics, pharmacodynamics and toxicology of theranostic nanoparticles. Nanoscale. 2015;7:18848–62.

16. Park GK, I H, Kim GS, Hwang NS, Choi HS. Optical spectroscopic imaging for cell therapy and tissue engineering. Appl Spectrosc Rev. 2018;53:360–75.

17. Sajedi S, Sabet H, Choi HS. Intraoperative biophotonic imaging systems for image-guided interventions. Nanophotonics. 2019;8:99–116.

18. Son J, Yi G, Yoo J, Park C, Koo H, Choi HS. Light-responsive nanomedicine for biophotonic imaging and targeted therapy. Adv Drug Deliv Rev. 2019;138:133–47.

19. Kim T, O'Brien C, Choi HS, Jeong MY. Fluorescence molecular imaging systems for intraoperative image-guided surgery. Appl Spectrosc Rev. 2018;53:349–59.

20. Hyun H, Park MH, Owens EA, Wada H, Henary M, Handgraaf HJ, et al. Structure-inherent targeting of near-infrared fluorophores for parathyroid and thyroid gland imaging. Nat Med. 2015;21:192–7.

21. Kim SH, Park G, Hyun H, Lee JH, Ashitate Y, Choi J, et al. Near-infrared lipophilic fluorophores for tracing tissue growth. Biomed Mater. 2013;8:014110.

22. Park GK, Lee JH, Levitz A, El Fakhri G, Hwang NS, Henary M, et al. Lysosome-targeted bioprobes for sequential cell tracking from macroscopic to microscopic scales. Adv Mater. 2019;31:e1806216.

23. Park MH, Hyun H, Ashitate Y, Wada H, Park G, Lee JH, et al. Prototype nerve-specific near-infrared fluorophores. Theranostics. 2014;4:823–33.

24. Hyun H, Owens EA, Wada H, Levitz A, Park G, Park MH, et al. Cartilage-specific near-infrared fluorophores for biomedical imaging. Angew Chem Int Ed Engl. 2015;54:8648–52.

25. Hyun H, Wada H, Bao K, Gravier J, Yadav Y, Laramie M, et al. Phosphonated near-infrared fluorophores for biomedical imaging of bone. Angew Chem Int Ed Engl. 2014;53:10668–72.

26. Tahmasebi S, Elahi R, Esmaeilzadeh A. Solid tumors challenges and new insights of CAR T cell engineering. Stem Cell Rev Rep. 2019;15:619–36.

27. Schroeder T. Imaging stem-cell-driven regeneration in mammals. Nature. 2008;453:345–51.

28. Choi HS, Liu W, Misra P, Tanaka E, Zimmer JP, Itty Ipe B, et al. Renal clearance of quantum dots. Nat Biotechnol. 2007;25:1165–70.

29. Arnhold S, Lenartz D, Kruttwig K, Klinz FJ, Kolossov E, Hescheler J, et al. Differentiation of green fluorescent protein-labeled embryonic stem cell-derived neural precursor cells into Thy-1-positive neurons and glia after transplantation into adult rat striatum. J Neurosurg. 2000;93:1026–32.

30. Siebert GA, Hung DY, Chang P, Roberts MS. Ion-trapping, microsomal binding, and unbound drug distribution in the hepatic retention of basic drugs. J Pharmacol Exp Ther. 2004;308:228–35.

31. Langer R, Vacanti JP. Tissue engineering. Science. 1993;260:920–6.

32. Atala A. Tissue engineering and regenerative medicine: concepts for clinical application. Rejuvenation Res. 2004;7:15–31.

33. Lee SJ, Van Dyke M, Atala A, Yoo JJ. Host cell mobilization for in situ tissue regeneration. Rejuvenation Res. 2008;11:747–56.

34. Hutmacher DW. Scaffolds in tissue engineering bone and cartilage. Biomaterials. 2000;21:2529–43.

35. Kim K, Jeong CG, Hollister SJ. Non-invasive monitoring of tissue scaffold degradation using ultrasound elasticity imaging. Acta Biomater. 2008;4:783–90.

36. Yang Y, Yiu HH, El Haj AJ. On-line fluorescent monitoring of the degradation of polymeric scaffolds for tissue engineering. Analyst. 2005;130:1502–6.

37. Choi HS, Gibbs SL, Lee JH, Kim SH, Ashitate Y, Liu F, et al. Targeted zwitterionic near-infrared fluorophores for improved optical imaging. Nat Biotechnol. 2013;31:148–53.

38. Choi HS, Nasr K, Alyabyev S, Feith D, Lee JH, Kim SH, et al. Synthesis and in vivo fate of zwitterionic near-infrared fluorophores. Angew Chem Int Ed Engl. 2011;50:6258–63.

39. Hyun H, Henary M, Gao T, Narayana L, Owens EA, Lee JH, et al. 700-nm zwitterionic Near-infrared fluorophores for dual-channel image-guided surgery. Mol Imaging Biol. 2016;18:52–61.

40. Katagiri W, Lee JH, Tétrault MA, Kang H, Jeong S, Evans CL, et al. Real-time imaging of vaccine biodistribution using zwitterionic NIR nanoparticles. Adv Healthc Mater. 2019;8:e1900035.

41. Kim H, Cho MH, Choi HS, Lee BI, Choi Y. Zwitterionic near-infrared fluorophore-conjugated epidermal growth factor for fast, real-time, and target-cell-specific cancer imaging. Theranostics. 2019;9:1085–95.

42. Kim KS, Hyun H, Yang JA, Lee MY, Kim H, Yun SH, et al. Bioimaging of hyaluronate-interferon alpha conjugates using a non-interfering zwitterionic fluorophore. Biomacromolecules. 2015;16:3054–61.

43. Kim KS, Kim YS, Bao K, Wada H, Choi HS, Hahn SK. Bioimaging of botulinum toxin and hyaluronate hydrogels using zwitterionic near-infrared fluorophores. Biomater Res. 2017;21:15.

44. Kim SH, Lee JH, Hyun H, Ashitate Y, Park G, Robichaud K, et al. Near-infrared fluorescence imaging for noninvasive trafficking of scaffold degradation. Sci Rep. 2013;3:1198.

45. Moroni L, Burdick JA, Highley C, Lee SJ, Morimoto Y, Takeuchi S, et al. Biofabrication strategies for 3D in vitro models and regenerative medicine. Nat Rev Mater. 2018;3:21–37.

46. Park GK, Kim SH, Kim K, Das P, Kim BG, Kashiwagi S, et al. Dual-channel fluorescence imaging of hydrogel degradation and tissue regeneration in the brain. Theranostics. 2019;9:4255–64.

47. Crema MD, Roemer FW, Marra MD, Burstein D, Gold GE, Eckstein F, et al. Articular cartilage in the knee: current MR imaging techniques and applications in clinical practice and research. Radiographics. 2011;31:37–61.

48. Ruan MZ, Dawson B, Jiang MM, Gannon F, Heggeness M, Lee BH. Quantitative imaging of murine osteoarthritic cartilage by phase-contrast micro-computed tomography. Arthritis Rheum. 2013;65:388–96.

49. Lim W, Kim B, Jo G, Yang DH, Park MH, Hyun H. Bioluminescence and near-infrared fluorescence imaging for detection of

metastatic bone tumors. Lasers Med Sci. 2019. https://doi.org/10.1007/s10103-019-02801-9.

50. Wu C, Wei J, Tian D, Feng Y, Miller RH, Wang Y. Molecular probes for imaging myelinated white matter in CNS. J Med Chem. 2008;51:6682–8.

51. Wu C, Tian D, Feng Y, Polak P, Wei J, Sharp A, et al. A novel fluorescent probe that is brain permeable and selectively binds to myelin. J Histochem Cytochem. 2006;54:997–1004.

52. Zhu S, Yung BC, Chandra S, Niu G, Antaris AL, Chen X. Near-infrared-II (NIR-II) bioimaging via off-peak NIR-I fluorescence emission. Theranostics. 2018;8:4141–51.